Spiraling into History: A Molecular Phylogeny and Investigation of Biogeographic Origins and Floral Evolution for the Genus *Costus*

Source: Systematic Botany, 40(1):104-115.
Published By: The American Society of Plant Taxonomists
URL: http://www.bioone.org/doi/full/10.1600/036364415X686404

Systematic Botany (2015), 40(1): pp. 104–115

DOI 10.1600/036364415X686404
Date of publication February 12, 2015

Spiraling into History: A Molecular Phylogeny and Investigation of Biogeographic Origins and Floral Evolution for the Genus *Costus*

Shayla Salzman,[1,2] Heather E. Driscoll,[1,3] Tanya Renner,[1,4] Thiago André,[1,5] Stacy Shen,[1] and Chelsea D. Specht[1,6]

[1]Departments of Plant and Microbial Biology and Integrative Biology and The University and Jepson Herbaria, 431 Koshland Hall, University of California, Berkeley, California 94720 U. S. A.
[2]Current address: Department of Organismic and Evolutionary Biology, 26 Oxford Street, Harvard University, Cambridge, Massachusetts 02138 U. S. A.
[3]Current address: Vermont Genetics Network, Department of Biology and Physical Education, Norwich University, Northfield, Vermont 05663 U. S. A.
[4]Current address: Center for Insect Science and the Department of Entomology, University of Arizona, Tucson, Arizona 85721 U. S. A.
[5]Current address: Laboratório Integrado de Sistemática Vegetal Departamento de Botânica, Av. Carlos Chagas Filho, 373, CCS A1-088, Universidade Federal do Rio de Janeiro, Rio de Janeiro 21941-902 Brazil.
[6]Author for Correspondence (cdspecht@berkeley.edu)

Communicating Editor: Donald H Les

Abstract—Rapid radiations are notoriously difficult to resolve, yet understanding phylogenetic patterns in such lineages can be useful for investigating evolutionary processes associated with bursts of speciation and morphological diversification. Here we present an expansive molecular phylogeny of *Costus* L. (Costaceae Nakai) with a focus on the Neotropical species within the clade, sampling 47 of the known 51 Neotropical species and including five molecular markers for phylogenetic analysis (ITS, *ETS*, *rps16*, *trnL-F*, and *CaM*). We use the phylogenetic results to investigate shifts in pollination syndrome, with the intention of addressing potential mechanisms leading to the rapid radiation documented for this clade. Our ancestral reconstruction of pollination syndrome presents the first evidence in this genus of an evolutionary toggle in pollination morphologies, demonstrating both the multiple independent evolutions of ornithophily (bird pollination) as well as reversals to melittophily (bee pollination). We show that the ornithophilous morphology has evolved at least eight times independently with four potential reversals to melittophilous morphology, and confirm prior work showing that neither pollination syndrome defines a monophyletic lineage. Based on the current distribution for the Neotropical and African species, we reconstruct the ancestral distribution of the Neotropical clade as the Pacific Coast of Mexico and Central America. Our results indicate an historic dispersal of a bee-pollinated taxon from Africa to the Pacific Coast of Mexico/Central America, with subsequent diversification leading to the evolution of a bird-pollinated floral morphology in multiple derived lineages.

Keywords—Ancestral state reconstruction, Costaceae, rapid radiation, Zingiberales.

Costus L. is a pantropical genus in the monocot family Costaceae. *Costus* is the most diverse genus within the Costaceae, with approximately 80 species in total. It comprises two main biogeographic groups; a paraphyletic assemblage of low-diversity clades native to tropical Africa and a large derived clade containing approximately 51 species and distributed exclusively in the Neotropics. The derived Neotropical clade appears to have arisen from a single long-distance dispersal event from Africa occurring approximately 34 million years ago (ma) (Specht 2006b). *Costus* species can be recognized by their characteristic monistichous spiral phyllotaxy, tubular sheathing leaf bases each with a pronounced ligule, and terminal (mostly) inflorescences with imbricate bracts arranged in several series of parastichies. While most species are terrestrial rhizomatous herbs, a few African species are epiphytic (*C. talbotii*, *C. lateriflorus*) and these have axillary rather than terminal inflorescences. *Costus* range in vegetative height from less than one meter to over 3 m tall. They tend to grow most abundantly in moist lowlands, wet thickets, clearings or streambeds at relatively low elevations (< 800 m), but some species have been collected at 2,000 m above sea level.

The evolution of two specific pollination syndromes sets *Costus* apart from other genera in the family (Kay 2006). Ornithophilous (hummingbird attracting) *Costus* have inflorescences constructed of mostly red, orange or yellow bracts and flowers with narrow, tubular openings. Melittophilous (bee attracting) *Costus* have mostly green-bracted inflorescences and flowers with a wider floral opening and a broad labellum that is white or yellow with distinct red or purple stripes forming a "landing platform" (Fig. 1). These morphologies have been shown to be consistent with hummingbird and bee pollination, respectively (Kay and Schemske 2003), and such morphology-based signaling appears to be more important than reward for defining pollination type, as both types of flowers produce copious nectar (see Thomson and Wilson 2008). Work done in Bornean gingers (Zingerberaceae and Costaceae) found no significant difference in sugar concentration between hummingbird- and bee-pollinated flowers but a highly elevated daily sugar production in hummingbird plants (Sakai et al. 1999). However, this has not been investigated within *Costus* alone. Previous work shows that bee pollination originally evolved in Africa and is ancestral to the Neotropical clade (Specht et al. 2001; Kay et al. 2005; Specht 2006b), and that hummingbird pollination is derived within the Neotropical clade and has evolved at least seven times independently (Specht 2006a).

It has been suggested that shifts in pollinator-specific morphologies may account for the rapid radiation seen in the Neotropical clade (Kay et al. 2005). Indeed, diversification rates within the New World *Costus* clade have been shown to be the second highest in the family, just behind the Asian genus *Tapeinochilos* Miq. (Specht 2005). Within Costaceae, *Tapeinochilos* is the only other genus with species displaying a distinct bird-pollination syndrome, associated with pollination by native sunbirds (O. Gideon pers. comm.).

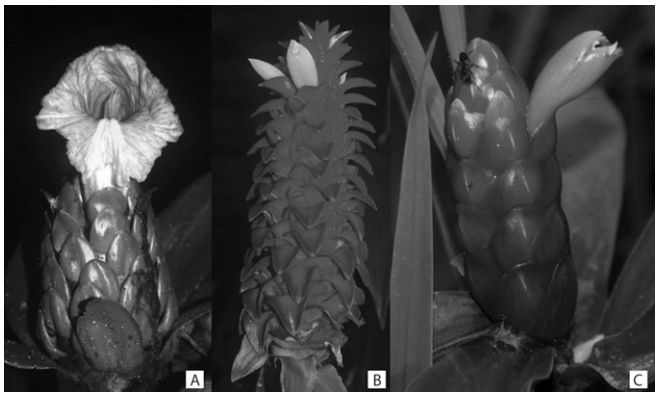

FIG. 1. Representative photos of Neotropical *Costus* species. (A) *Costus guanaiensis* Rusby var. *guanaiensis* showing the melittophilous morphology. (B) *Costus comosus* and (C) *Costus scaber* showing the ornithophilous morphology. Photos by C. D. Specht.

Fossil-calibrated molecular dating analyses using chloroplast markers (*trnL-F* and *trn*K) put the diversification of *Costus* at around 40 ma with early-diverging lineages occurring exclusively in Africa and maintaining a plesiomorphic floral morphology that is not specifically associated with either bee or hummingbird pollination (Specht 2006b). Melittophilous *Costus* are suggested to have evolved around 34 ma. One of these melittophilous *Costus* dispersed to the New World, and the fossil-calibrated dating places the New World radiation at around 22 ma (Specht 2006b) with both floral forms present by 20 ma. An ITS molecular clock analysis suggests that the Neotropical diversification occurred much more rapidly, with the ca. 50 species diversifying within the last four million years (Kay et al. 2005). Parsimony ancestral state reconstruction using broad geographic species ranges placed the dispersal from Africa to Central America (Kay et al. 2005).

Here we present a phylogenetic hypothesis for the genus *Costus* with expanded taxon sampling, including 47 of approximately 51 Neotropical taxa, and increased character sampling including chloroplast (*rps16*, *trnL-F*), nuclear (*CaM*), and nuclear ribosomal (ITS, ETS) molecular data. We analyze ancestral pollination syndromes using Bayesian, maximum parsimony, and maximum likelihood approaches and investigate biogeographic patterns of dispersal and vicariance using narrowly defined geographic ranges for ancestral area reconstruction. We confirm the multiple independent origins of the melittophilous and ornithophilous morphologies, and show the first evidence for reversal from ornithophilous to melittophilous morphology. We hypothesize that the origin and evolution of these specific pollination-driven morphologies are important contributors to the rapid radiation seen in this clade.

Materials and Methods

Taxon Sampling—Seventy-four *Costus* individuals were selected in an attempt to sample broadly within the genus. To provide a strong and robust outgroup, seven individuals representing all other genera in Costaceae were included. Leaf tissue collected from the field (collectors P. J. M. Maas, D. Skinner, and C. D. Specht) was supplemented by sampling live tissue from living collections at the New York Botanical Garden, the UC Botanical Garden at Berkeley, Lyon Arboretum, and the Smithsonian Greenhouse's living collection. All newly acquired sequences are deposited in GenBank with vouchered collection information (Appendix 1).

DNA Sequence Data and Analysis—DNA was extracted from silica-dried leaf material using Edwards et al.'s (1991) method. The PCR fragments were generated for two chloroplast markers (*rps16* partial coding sequence with partial *trn*k-*rps16* intergenic spacer and *trnL-F* intergenic spacer with partial tRNA-Leu and tRNA-Phe genes), one nuclear gene (partial first intron and partial coding sequence of calmodulin (*CaM*)), and two transcribed spacer regions of the ribosomal DNA array (ITS and ETS) using Phire hot start II DNA polymerase (Thermo Fisher Scientific, Pittsburgh, Pennsylvania) with a 3 min initial denaturing step at 98 °C, 45 cycles of 5 sec at 98 °C, 15 sec at gene-specific annealing temperatures, and 20 sec at 72 °C, and a final 1 min 72 °C extension. For ETS, 45 cycles included 5 sec at 98 °C followed by 20 sec at 72 °C for a combined anneal and extension. Table 1 lists primer pairs and specific annealing temperatures. The *CaM* primers were designed for this study following cloning and sequencing of PCR products amplified with the Zingiberales-specific primers cam33F and the reverse complement of cam328R (Johansen 2005). Cycle sequencing was performed using BigDye v3.1 (Applied Biosystems, Foster City, California) following manufacturer's protocol. Sequencing was done at the UC Berkeley Museum of Vertebrate Zoology's Evolutionary Genetics Laboratory (EGL) on an Applied Biosystems 3730xl DNA analyzer. Reads were assembled and edited and multiple sequence alignments generated in Geneious (v5.6.3) using the Geneious alignment algorithm. Manual alignment editing was done in Geneious (v5.6.3) and Mesquite (Maddison and Maddison 2011).

Phylogenetic Analysis—A concatenated alignment with a total of 4,654 characters containing ITS, ETS, *CaM*, *rps16*, and *trnL-F* sequences was used to generate phylogenetic hypotheses under maximum likelihood (ML), maximum parsimony (MP), and Bayesian inference methods. Gaps and the ends of shorter sequences were treated as missing data. Models of evolution were determined for each marker alignment as well as the full concatenated alignment by jModelTest v0.1.1 (Darriba et al. 2012) using Bayesian information criterion. Character statistics and models of evolution for all alignments are listed in Table 2. Individual marker trees were run using the appropriate models in PhyML as implemented in Geneious (v5.6.3) and MrBayes (v3.2; Ronquist and Huelsenbeck 2003) using the CIPRES Scientific Gateway (Miller et al. 2010). The MCMC parameters for each analysis include 100,000,000 generations using four chains, a cold chain temperature of 0.2, tree sampling every 1,000, and variable site-specific rate models of: two substitution types and gamma distributed rate variation with a proportion of invariable sites for ITS, six substitution

TABLE 1. Primer pairs and annealing temperatures used in this study. Primers were used for both amplification and sequencing.

	5′-3′	Annealing	Reference
ITS Leu F	GTCCACTGAACCTTATCATTTAG	59.3	Baum et al. 1998
ITS 4	TCCTCCGCTTATTGATATGC		White et al. 1990
ETS Costus F	CTTTGTTGTGCTCGGCGGAGTTC	72	Kay et al. 2005
18S-IGS	GAGACAAGCATATGACTACTGGCAGGATCAACCAG		Baldwin and Markos 1998
CaM Costus F	TGCTTCTCTCGAACGCTAGAT	66	This study
CaM Costus R	GAAACTCGGAATGCCTCCTT		This study
rps16x2F2	AAAGTGGGTTTTTATGATCC	57.5	Shaw et al. 2007
trnKx1	TTAAAAGCCGAGTACTCTACC		Shaw et al. 2007
trnLc	CGAAATCGGTAGACGCTACG	67	Taberlet et al. 1991
trnFf	ATTTGAACTGGTGACACGAG		Taberlet et al. 1991

Table 2. Character values and models of evolution for each marker and the concatenated alignment.

Marker	Number of Characters	Proportion of Missing Data	Parsimony-Informative Characters	Constant Characters	Model of Evolution
ITS	841	0.0958	219	393	K80 + I + G
ETS	651	0.1228	291	210	TPM2uf + G
CaM	818	0.1207	247	381	TPM3 + I
*rps*16	1,164	0.1270	45	924	TPM1uf + G
trnL-F	1,180	0.1230	59	949	TPM1uf + I + G
Concatenated	4,654	0.1191	861	2,857	TIM3 + G

types with proportion of sites invariable for *CaM*, and six substitution types with gamma distributed rate variation for ETS, *rps16*, and *trnL-F*. Runs were stopped early if a convergence diagnostic of 0.01 was met. A consensus tree for each single marker analysis was generated using the sumtrees command with a minimum clade frequency of 50% and after a burn-in of 10% as determined by visualizing posterior distributions of the parameter values in Tracer (v1.5; Rambaut and Drummond 2007). Five separate ML analyses were performed on the full concatenated alignment in PhyML (Guindon et al. 2010) using TIM3 + G with random starting trees, random sequence addition, and SPR topology searches. Additionally, to assess clade support 1,000 ML bootstrap replicates were run using TIM3 + G in PhyML as implemented in Geneious (v5.6.3). The MP analysis was conducted in PAUP* v4.0b10 (Swofford 2003) using 1,000 replicates of random sequence addition, TBR topology searches, and holding up to 1,000 trees per replicate. Parsimony bootstrap replications (1,000) with ten replicates each of random sequence addition and TBR searching were also performed in PAUP*. A partitioned Bayesian analysis was performed on the concatenated alignment using the same models for each partition as described for individual marker analyses and the same MCMC parameters, with the exception of the temperature parameter (here set to 0.1). A consensus tree was generated using the sumtrees command with a minimum clade frequency of 50% and after a burn-in of 10% as determined by visualizing posterior distributions of the parameter values in Tracer (v1.5; Rambaut and Drummond 2007). Phylogenetic analyses and alignments are accessible on TreeBASE (study number TB2:S16238).

Ancestral State Reconstruction Analysis—The topology recovered in the ML analysis (Fig. 2) was used for reconstructing ancestral character states for pollination syndrome and to reconstruct ancestral areas based on current distributions. The Bayesian phylogeny showed a slightly different topology (discussed below) and was also used for ancestral state reconstruction; in this case, polytomies were resolved to have branch lengths of 0 prior to analyses using the Mesquite command "resolve polytomies." Pollination type was coded as generalist, bee, or bird based on the pollination syndrome morphologies tested by Kay and Schemske (2003; Fig. 1). Models of pollination rate shift variation were tested in BayesTraits (Pagel and Meade 2004a). All rate shifts were found to be independent. Shifts between generalist and bee or between generalist and bird were below 10 and shifts between bee and bird were above 100. Ancestral state reconstruction for pollination syndrome was tested using a ML approach. Rates were permitted to be independent and vary in both Mesquite using StochChar model Mk1 with a decision threshold of 2.0 (Maddison and Maddison 2006) and in BayesTraits using BayesMultiState (Pagel et al. 2004). Bayesian reconstruction was also tested in BayesTraits using BayesMultiState with 5,050,000 generations with sampling every 300. A prior of uniform distribution of 0–10 was designated for rates between generalist pollination and either bird or bee, while a prior of uniform distribution of 50–150 was set for rates between bee and bird. The rate deviation was set to 15 so as to allow for an acceptance rate of around 20% for new models with each generation. Bayesian results were tested for statistical significance using the Bayes factor test of twice the difference between the harmonic means of runs, where the node in question was forced as bee and then as bird pollination. Any positive value favors the model; a value greater than (>) two is positive evidence, > five is strong evidence, and > 10 is very strong evidence for the model. Similarly, the significance of likelihood values given in BayesTraits analyses were tested using the likelihood ratio test. A significant result is defined as the difference of at least two log likelihood scores between runs when the node in question was forced as either bee or bird pollination (Pagel 1999).

Current distributions for all *Costus* species sampled were assembled as point data using locality data from the Global Biodiversity Information Facility (GBIF), and point data were coded as pertaining to any of 14 individual geographic ecoregions (Olson et al. 2001; see map, Fig. 2). Data points from GBIF were culled from inclusion (assumed erroneous) when only one collection for a given species was found in any particular ecoregion, unless the collection was positively identified and expertly curated. Ancestral distribution was tested with statistical dispersal-vicariance analysis (S-DIVA) (Yu et al. 2010) and Bayesian analyses in reconstruct ancestral state in phylogenies (RASP) (Yu et al. 2012). The S-DIVA reconstruction was set to a maximum of four possible ancestral distribution areas and the bound and hold values were allowed to be the maximum. RASP's Bayesian binary method includes two models, the fixed character state JC model and the estimated character state F81 model. As distributions gathered from GBIF are extensive yet may not cover the breadth of distribution, both were tested with and without gamma distribution. All runs used a wide root distribution at 50,000 generations, sampling every 100, using 10 chains, with a cold chain temperature of 0.1 and a maximum of four possible ancestral distribution areas. Additionally, elevations were acquired for the GBIF data points using ArcGIS 9.3 elevation and imagery data and tested for correlation with pollination syndrome using BayesTraits (Pagel et al. 2004). A MCMC of 1,010,000 generations was run twice using a continuous random walk model with autotune rate deviation and a uniform prior of 0–1,500 for alpha-elevation and a uniform prior of 0–2 for alpha-pollination. The two runs were compared after a burn-in of 10,000 and the significance of positive or negative correlation was tested with the Bayes factor test.

Diversification Analysis—The topology recovered in the ML analyses was tested for shifts in diversification rates using Bayesian analysis of macroevolutionary mixtures (BAMM) version 2.0.0 (Rabosky 2014) and analyzed using BAMMtools version 1.0.1 (Rabosky et al. 2014). The ML tree was first trimmed of outgroup taxa and made ultrametric using the R package ape version 3.1–2 (Paradis et al. 2004). Bayesian priors for BAMM were determined with setBAMMpriors in BAMMtools. 1,000,000,000 generations were tested for convergence with the coda package (Plummer et al. 2006) in R after a burn-in of ten percent.

Results

Molecular Data and Phylogenetic Inference—Single-marker Bayesian and ML trees show similar assemblages of African *Costus* taxa and a monophyletic Neotropical clade (data available in TreeBASE TB2:S16238). However, relationships among African clades and within Neotropical *Costus* are unresolved and/or poorly supported in most single marker topologies. Despite some discordance at the single-marker level, well supported nodes were largely congruent and the cumulative signal from the concatenated data yielded well-supported trees in Bayesian and ML analyses. As a result, a multi-marker approach was favored to maximize phylogenetic information (Smith 2000). The following results and discussion are based on analyses using the concatenated alignment.

The ML tree (one of five topologically identical random starts maximum likelihood trees of a concatenated alignment of ITS, ETS, *CaM*, *trnL-F*, and *rps16* using TIM3 with gamma distribution) has a log-likelihood of -23,899.35952 (Fig. 2). The 1,000 replication ML bootstrap consensus tree,

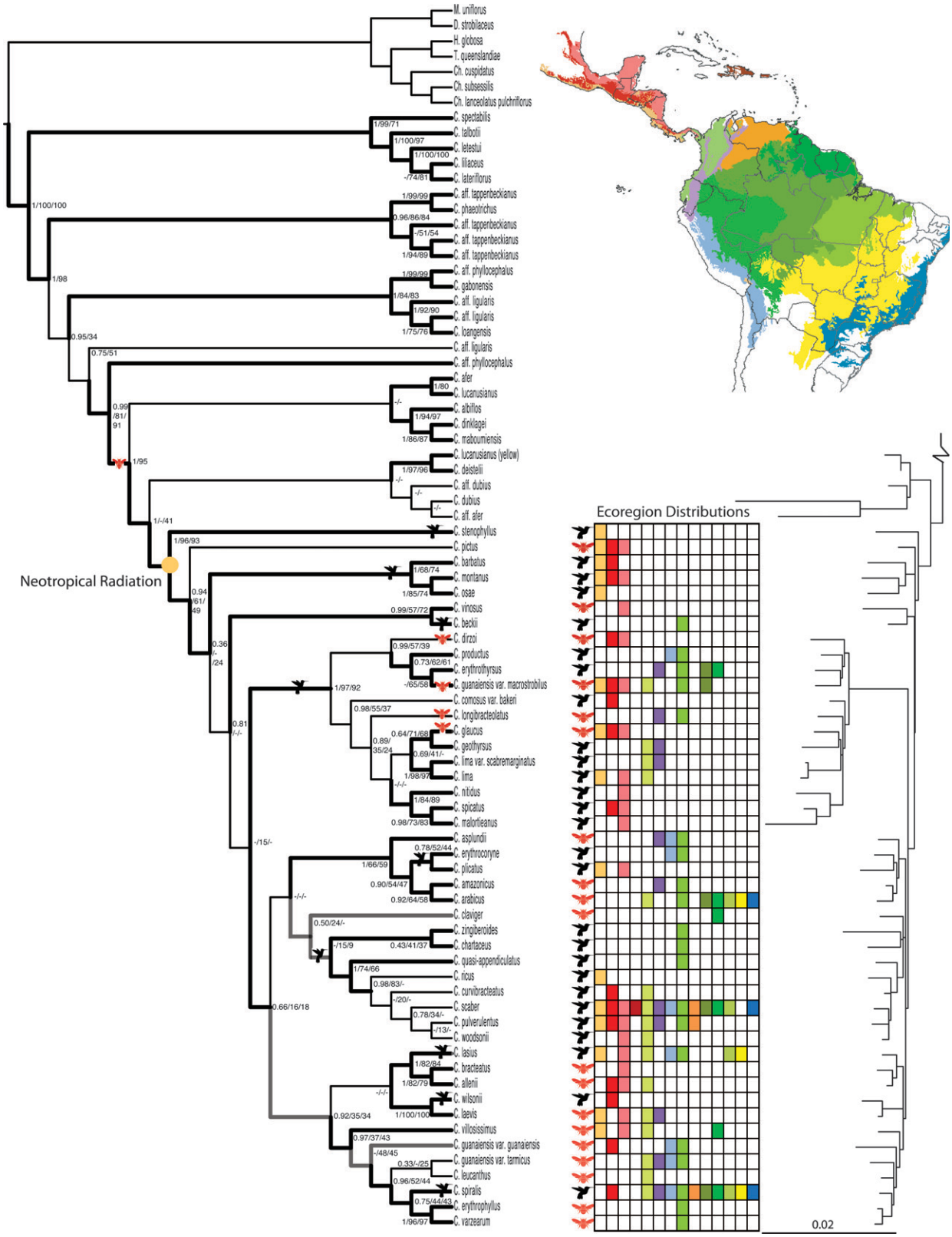

FIG. 2. Maximum likelihood hypothesis for Neotropical *Costus*. ML cladogram (with support values) showing character state reconstruction data and phylogram (with branch lengths) for the concatenated alignment of ITS, ETS, *CaM*, *rps16*, and *trnL-F* using TIM3 with gamma distribution and log likelihood score of -23,944. Support values at nodes are Bayesian posterior probabilities, ML, and MP bootstrap proportions. Nodes supported by a PAUP* strict consensus of 707,000 most parsimonious trees are shown in bold with 50% consensus in bold grey. Distributions were obtained from herbaria records housed in the Global Biodiversity Information Facility. Ecoregions are based on the World Wildlife Fund's ecoregion designations (Olson et al. 2001). Ancestral distribution for the Neotropical clade indicated (Pacific Coast of Mexico and Central America) based on S-DIVA and MCMC algorithms implemented in RASP. ML reconstructions performed in Mesquite and BayesTraits are indicated: shifts to ornithophilous morphology are denoted with hummingbirds and shifts to melittophilous morphology denoted with bees. Extant pollination syndromes are denoted with hummingbirds or bees at tips.

using TIM3 with gamma distribution, gave largely the same topology with low bootstrap support scattered across the Neotropical *Costus* clade.

The MP analysis of the full data set resulted in 707,000 most parsimonious trees with a score L = 3,027. A strict consensus of these trees supports a number of clades (Fig. 2, bold) with further 50% consensus support (Fig. 2, bold grey). The parsimony bootstrap obtained low support values scattered across the tree, however overall the topology does not disagree with the ML tree with the exception of a few relationships discussed below.

The combined Bayesian analysis shows an average standard deviation of split frequencies between the two runs of 0.0047 at 100,000,000 generations. After a burn-in of 10%, the remaining 180,020,000 trees have a mean log likelihood of -22,178.236 with an effective sample size of 17,281. All other statistics between runs have mean values with effective sample sizes greater than 16,500. The topology reconstructed by Bayesian analysis largely supports the ML tree. The exceptions are discussed further below.

Phylogenetic Relationships—*Costus* is reconstructed as monophyletic, with African species forming numerous small clades as early-diverging lineages (Figs. 2, 3). The New World clade is monophyletic and sister to a clade of African taxa (including several accessions of *C. dubius*) with a bee-pollinated floral morphology.

Small differences in relationships suggested by each of the phylogenetic methods make clear that further nucleotide sampling is necessary to completely resolve species relationships within the *Costus* lineage. However, questions regarding ancestral distribution and pollination shifts in the Neotropical clade can be addressed given the resolution acquired. Taxa or accessions that show different placement or form polytomies when using different inference methods are discussed below.

Within the Old World lineages, one accession of *C. dubius* is strongly supported as sister to the *C. albiflos*/*C. maboumiensis* clade in the Bayesian reconstruction (Fig. 4) and in the MP strict consensus tree (data not shown). The same accession of *C. dubius* is reconstructed as part of a clade with other potential *C. dubius* accessions (*C.* aff *dubius*, *C.* aff *afer*) in all ML runs (Figs. 2, 3), indicating that the individual accession may be of hybrid origin. The other two accessions identified as having affinity with *C. dubius* form a clade with *C. lucanusianus* and *C. deistelii*, and it is this clade that is sister to the New World radiation.

Within the Neotropical lineage, the clade formed by *C. vinosus* and *C. beckii* is weakly supported as sister to the *C. dirzoi*/*C. malortieanus* clade in parsimony (BS 21%) and Bayesian (PP 0.62) analyses. Interestingly, however, these two taxa are placed as sister to the remainder of the New World clade in the ML tree. While *C. longebracteolatus* clearly belongs in the *C. glaucous*/*C. malortieanus* clade as supported by all methods, its exact placement is unresolved. Similarly, the placement of the *C. asplundii*/*C. arabicus* clade is unresolved, as Bayesian and ML bootstrap methods very weakly support it as sister to the *C. claviger*/*C. woodsonii* clade (0.22 posterior probability and 16% respectively), while parsimony methods maintain a polytomy among these taxa. Finally, it is unclear if the *C. laevis*/*C. wilsonii* clade is indeed sister (ML) to the *C. lasius*/*C. allenii* clade, as other inference methods very weakly support it as sister to the larger *C. lasius*/*C. varzearum* clade (0.35 PP, MLBS 35%, MPBS 19%).

We feel most confident with the topology represented in the ML tree as, in the four cases discussed, only the *C. vinosus*/*C. beckii* clade shows a different placement altogether. The other three cases resolved in the ML tree are merely unresolved with other methods, which could be expected as rapid radiations may not have sufficient data to inform the priors in Bayesian analysis. However, because these differences were seen between the ML tree and the Bayesian tree, ancestral pollination reconstruction was run on both, specifically to investigate if the placement of the *C. vinosus*/*C. beckii* clade would affect the number of hypothesized ancestral character state shifts in pollination syndrome.

Ancestral Character State Reconstruction: Pollination Syndromes—A presumed generalist pollination morphology is recovered as ancestral to the genus, with a monophyletic shift to a melittophilous morphology within the Old World grade (Figs. 3, 4). We recognize that generalist pollination used as the plesiomorphic state may reflect a lack of knowledge of the pollination biology of the early-diverging lineages within the Costaceae (ex. *Dimerocostus*, *Monocostus*, and *Chamaecostus*), which have been historically treated as generalists because pollination syndromes based on flower morphology are not conclusive for these lineages, as with the melittophilous and ornithophilous pollination syndromes of *Costus* tested by Kay and Schemske (2003). The monophyletic New World clade was reconstructed as being ancestrally melittophilous, despite the resolution of ornithophilous taxon *C. stenophyllus* as the sister to all remaining Neotropical *Costus*: this result indicates that bird pollination evolved in *C. stenophyllus* after it diverged from the remaining taxa. Based on our recovered topology, there have been up to nine shifts to hummingbird pollination morphology from the bee-pollinated ancestral form, with four reversals to a bee pollination syndrome (Fig. 2). Pollination syndromes were weakly correlated with elevations. The MCMC run showed an average correlation coefficient, R, of 0.2 with a standard deviation of 0.01. This correlation is positively supported with a Bayes factor of 2.78.

Pollination Syndromes Reconstructed on ML Phylogeny—Overall, reconstruction of ancestral character states on the ML tree recover much stronger statistical significance for nodes tested than are recovered on the Bayesian tree. The ML pollination syndrome reconstruction tree (Fig. 3) has a negative log likelihood of 69.57 and a rate of 21.479 as determined by the Mk1 model in Mesquite. Bayesian runs had an average acceptance rate of new models for each generation of 19% showing ideal mixing of chains. Reconstruction with Mesquite supports nodes along the backbone as statistically significant for both ornithophilous and melittophilous morphologies even with moderately high likelihoods pointing to bee pollination. Reconstructed ancestral morphologies of the more derived clades, except for *C. chartaceus*/*C. woodsonii* (discussed below), are statistically supported as follows: hummingbird pollination syndrome for the ancestor of the clade containing *C. dirzoi*/*C. lima*; hummingbird for *C. dirzoi*/*C. erythrothyrsus*; hummingbird for *C. comosus* var. *bakeri*/*C. lima*; and bee pollination syndrome morphology for the ancestor of *C. laevis*/*C. varzearum* (Fig. 3). The Bayes factor positively supports all tested nodes with Bayes factors greater than 2 except for the ancestor of *C. chartaceus* and *C. woodsonii*. However, this ancestor's posterior probability of 0.95 for the hummingbird

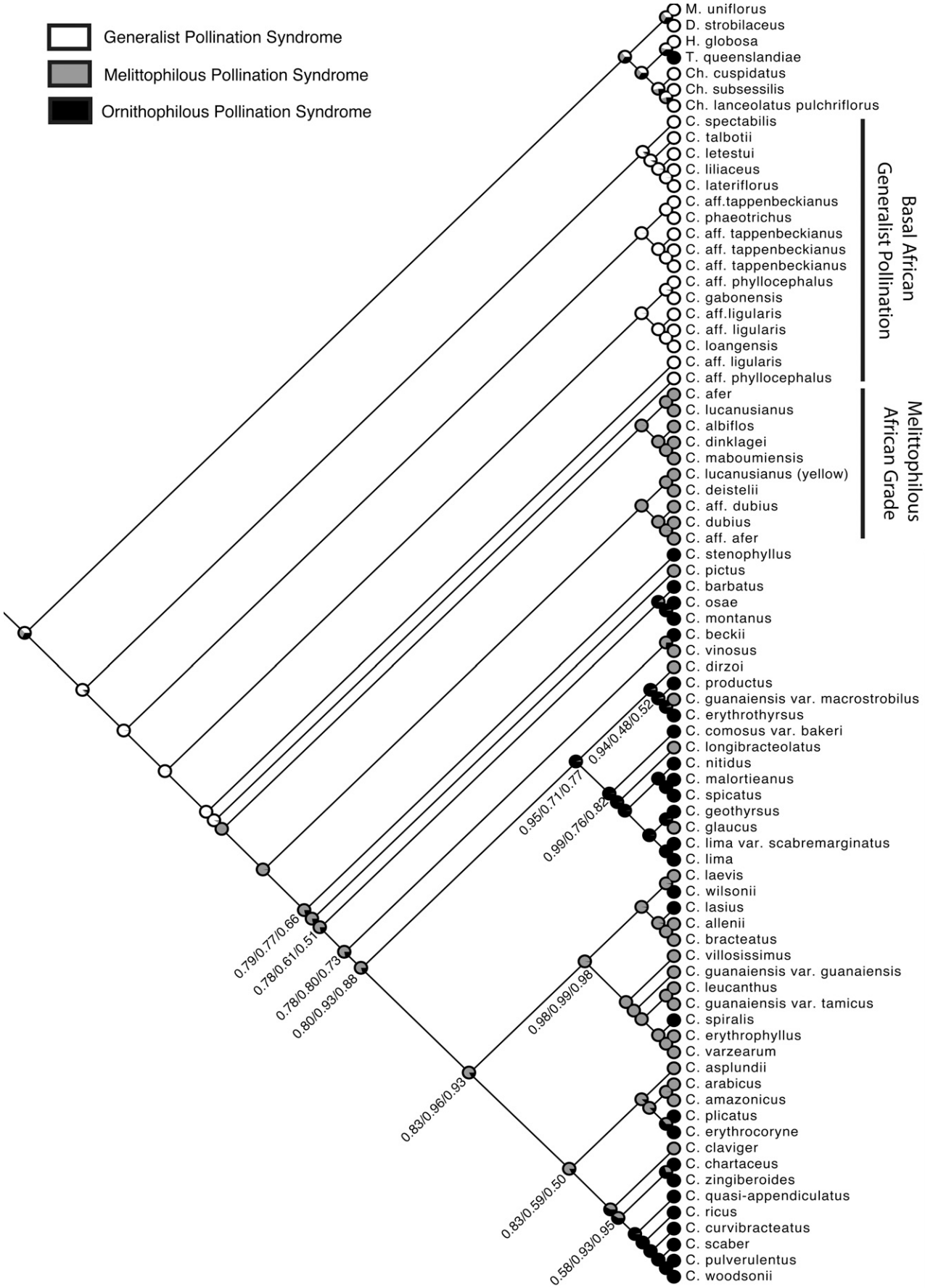

FIG. 3. Reconstruction of ancestral character states for morphology-based pollination syndrome on ML tree. Generalist, melittophilous and ornithophilous morphologies are indicated with likelihood support values from Mesquite and BayesTraits and posterior probabilities from BayesTraits.

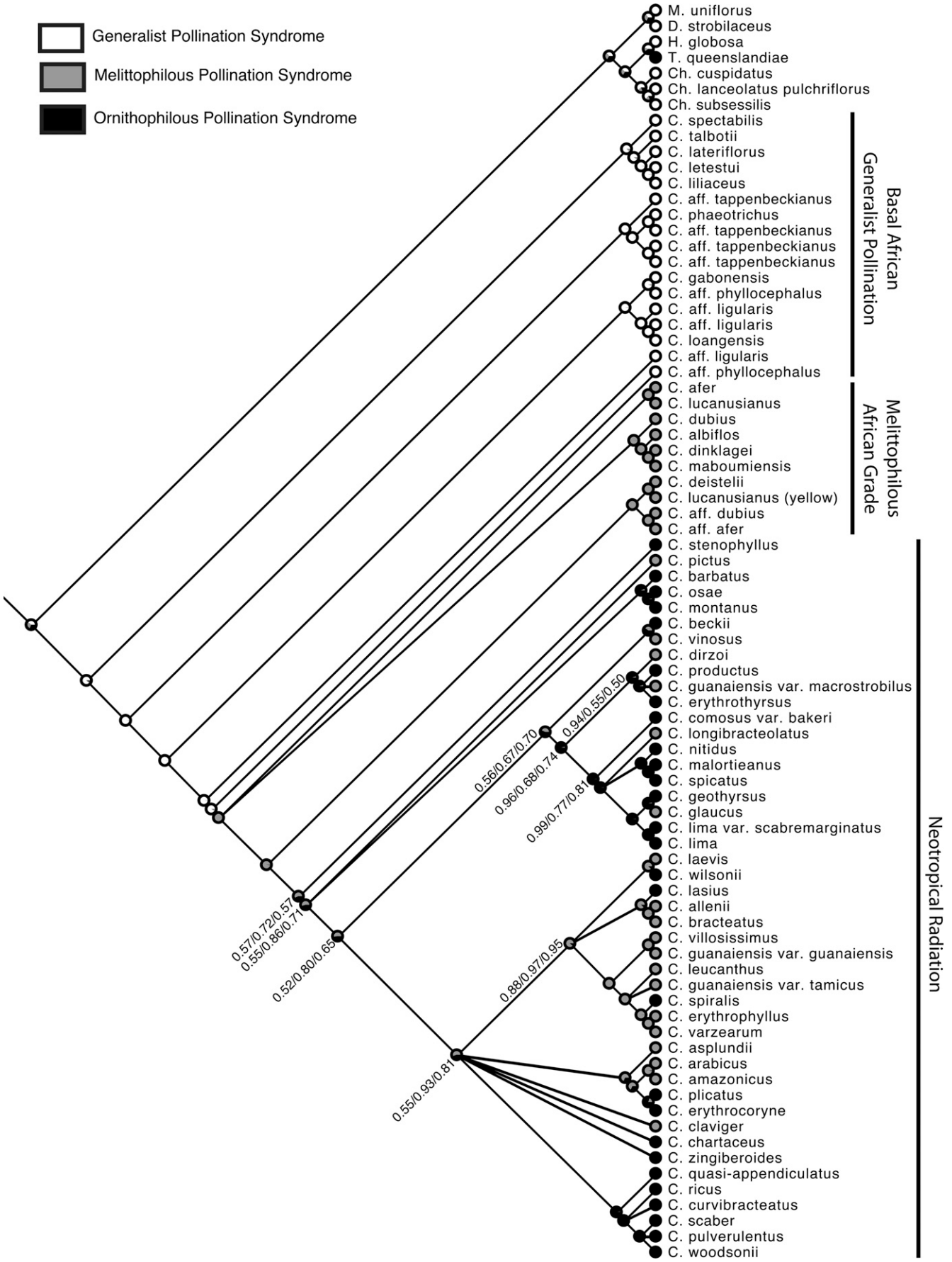

FIG. 4. Reconstruction of ancestral character states for morphology-based pollination syndrome on Bayesian tree. Generalist, melittophilous, and ornithophilous morphologies are indicated with likelihood support values from Mesquite and BayesTraits and posterior probabilities from BayesTraits.

TABLE 3. BayesTraits ML probabilities, Bayesian posterior probabilities, and their support values at each node tested for ancestral pollination reconstruction using the ML tree. Nodes supported as having ancestral hummingbird pollination morphology are underlined.

Most Recent Common Ancestor of:	ML Probability (Bee)	ML Probability (Bird)	Δ log-likelihood	Posterior Probability (Bee)	Posterior Probability (Bird)	Bayes Factor
stenophyllus/woodsonii	0.77	0.23	1.76	0.66	0.34	3.11
barbatus/ woodsonii	0.61	0.39	1.89	0.50	0.50	3.22
beckii/ woodsonii	0.80	0.20	1.90	0.73	0.27	3.32
dirzoi/ woodsonii	0.93	0.07	2.33	0.88	0.12	4.11
dirzoi/lima	0.28	0.72	0.88	0.23	0.77	18.92
dirzoi/erythrothyrsus	0.52	0.48	0.78	0.48	0.52	2.12
comosus v. *bakeri/lima*	0.23	0.76	1.07	0.19	0.81	2.99
laevis/ woodsonii	0.97	0.03	2.59	0.93	0.07	4.78
laevis/varzearum	0.99	0.01	3.10	0.98	0.02	6.85
asplundii/ woodsonii	0.59	0.41	2.61	0.50	0.50	4.72
chartaceus/ woodsonii	0.07	0.93	1.25	0.05	0.95	1.88

morphology is highly supported (Bayes factor =1.88) and all extant taxa in this clade display a hummingbird pollination morphology (Fig. 3; Table 3). The ancestor of *C. dirzoi* and *C. lima* shows very strong evidence for having a hummingbird pollination morphology (Bayes factor = 18.92; posterior probability = 0.77; Mesquite likelihood reconstruction = 0.95), but interestingly, has only moderate support from BayesTraits likelihood reconstruction (delta log-likelihood = 0.88; likelihood = 0.72). In fact, the three nodes tested in this *C. dirzoi*/*C. lima* clade are supported as ornithophilous with Mesquite's likelihood reconstruction, Bayes factor test and BayesTraits (Fig. 3; Table 3). All three of these methods tested on the ML tree support a total of nine shifts to the ornithophilous pollination syndrome with four reversals to a melittophilous pollination syndrome in the *C. dirzoi*/*C. lima* clade.

POLLINATION SYNDROMES RECONSTRUCTED ON BAYESIAN PHYLOGENY—The Mesquite ML reconstruction on the Bayesian tree (Fig. 4) has a log likelihood of 69.02 and a rate of 20.96 as determined by the Mk1 model. Bayesian runs had an average acceptance rate of new models for each generation of 21% again showing ideal mixing of chains. Mesquite counts all nodes values as statistically significant for both hummingbird and bee morphologies, supporting neither as exclusive, except for the three ancestors tested within the *C. dirzoi*/*C. lima* clade, which are all statistically significant for hummingbird pollination morphology. ML methods in BayesTraits only show strong statistical support for the ancestor of *C. laevis* and *C. varzearum* as having bee pollination morphology, with moderate to high support for bee pollination morphology in the ancestors of *C. stenophyllus/C. woodsonii*, *C. pictus/C. woodsonii*, *C. beckii/C. woodsonii*, and *C. laevis/C. woodsonii* (Fig. 4; Table 4). Bayesian posterior probabilities at nodes tested in BayesTraits, however, are all favorably supported with Bayes factors greater than 2, except where there is positive support for hummingbird pollination morphology in the ancestor of *C. beckii* and *C. lima* (Bayes factor =1.40, posterior probability = 0.70) and an equal probability of hummingbird or bee pollination syndrome morphologies in the ancestor of *C. dirzoi* and *C. erythrothrysus* (Table 4). The differing topology seen in the Bayesian tree regarding the placement of *C. beckii* (hummingbird) and *C. vinosus* (bee) as sister to the *C. dircoi/C. lima* clade, strongly reconstructed as having a hummingbird pollination syndrome as the ancestral morphology on the ML tree, reduced the number of shifts to ornithophilous morphology to eight and increased the number of reversals to five with low support (Fig. 4; Table 4).

Reconstruction of Ancestral Distribution—S-DIVA as implemented in RASP with a maximum of four possible areas gives a relative probability = 1.00 for the Pacific Coast of Mexico and Central America as the combined ancestral area for Neotropical *Costus* (light yellow area on map, Fig. 2). The Bayesian binary method was run four times, once with each model, all of which point to a Mexican/Central American origin in the New World, with the strongest probability of being located along the Central American Pacific Coast (CAPC; Fig. 2 light yellow), and much smaller probabilities associated with distributions along the Central American Atlantic Coast (CAAC; Fig. 2 pink), or the Central American Interior (CAI; Fig. 2 red). After 50,000 generations, the F81 model had a distance between runs of 0.0049 and

TABLE 4. BayesTraits ML probabilities, Bayesian posterior probabilities, and their support values at each node tested for ancestral state reconstruction of pollination syndrome using the Bayesian topology. Nodes supported as having ancestral hummingbird pollination syndrome morphology are underlined.

Most Recent Common Ancestor of:	ML Probability (Bee)	ML Probability (Bird)	Δ log-likelihood	Posterior Probability (Bee)	Posterior Probability (Bird)	Bayes Factor
stenophyllus/ woodsonii	0.72	0.28	1.71	0.57	0.43	2.67
pictus/ woodsonii	0.86	0.14	1.75	0.71	0.29	2.73
beckii/ woodsonii	0.80	0.20	1.56	0.65	0.36	2.36
beckii/lima	0.33	0.67	1.07	0.30	0.70	1.40
dirzoi/lima	0.32	0.68	0.62	0.26	0.74	2.23
dirzoi/erythrothrysus	0.56	0.44	0.56	0.50	0.50	1.83
comosus v. *bakeri/lima*	0.23	0.77	0.70	0.20	0.80	2.92
laevis/ woodsonii	0.93	0.07	1.72	0.82	0.18	2.72
laevis/varzearum	0.97	0.03	2.27	0.95	0.05	4.26

gave the probabilities of the ancestral distribution at the Neotropical node (indicated Fig. 2) as CAPC = 69.48%, CAPC plus CAAC = 5.12%, Old World = 5.17%, and CAPC plus Old World = 8.69%. F81 with gamma distribution had a distance between runs of 0.0056 and probabilities of CAPC = 36.58%, CAPC plus CAI = 12.90%, CAPC plus CAAC = 10.64%, CAI = 9.87%, and CAAC = 8.14%. The JC model had a distance between runs of 0.0060 and probabilities of CAPC = 66.39%, CAPC plus Old World = 11.05%, Old World = 8.46%. The JC model with gamma distribution had a distance of 0.0073 and probabilities of CAPC = 48.23%, CAPC plus CAI = 13.67%, CAI = 8.20%, and CAPC plus CAAC = 7.98%. These methods all support a Mexican/Central American origin with the Pacific Coast as the most likely area of ancestral distribution (Fig. 2; light yellow).

***Diversification Analysis*—**Increased rates of speciation seen in *Costus* appear to be correlated with specialized pollination morphology. The mean lambda for the clade of all ornithophilous and melittophilous species (*C. afer*/*C. varzearum*) is 78.3732 with a 90% highest density probability (HDP) of 59.23909–100.95127. This is a large increase over the relative rate for species with generalist pollination morphology: 7.680111 (HPD 3.87069–13.64808). The Neotropical clade is further increased with a mean lambda of 205.4129 (HDP 156.0841–261.9265). Sub-clades within the Neotropical clade do not show relative rate differences regardless of pollination morphologies present in the clade. The hummingbird-pollinated clade of *C. chartaceus*/*C. woodsonii* has a mean lambda of 434.3955 (HDP 333.0779–558.5928) where the mostly bee-pollinated clade of *C. laevis*/*C. varzearum* has 434.322 (HDP 332.7832–558.0226). The *C. dirzoi*/*C. lima* clade with reversals to melittophilous morphology has a similar mean lambda of 434.2816 (HDP 332.6214–557.7095).

Discussion

Here we have presented a phylogeny for the genus *Costus* that shows the first evidence of an evolutionary toggle between hummingbird and bee pollination morphologies among species in the Neotropical clade. This expanded taxon and molecular marker phylogeny supports prior work showing that there have been multiple shifts in pollination syndromes in the genus. The increased sampling and resolution provided in this study suggests a greater number of origins of hummingbird pollination and finds for the first time the reversal from ornithophilous to melittophilous morphology, laying the ground work for further discussion of the factors related to the rapid radiation observed in this clade.

Phylogenetic inference is notoriously difficult for groups that have undergone rapid radiations, and even the use of rapidly evolving ribosomal spacers and a nuclear intron did not provide sufficient phylogenetic signal to resolve all evolutionary relationships within this lineage with strong support. ML analyses, however, resulted in a single topology that was largely reproduced with a 50% majority rule parsimony tree, excepting only a few close relationships that were unresolved in parsimony. Bayesian methods supported the same topology except, again, for a few unresolved polytomies and the placement of the *C. vinosus*/*C. beckii* clade, which was resolved with low support (0.54 posterior probability). Despite these phylogenetic uncertainties, hypotheses regarding shifts in pollination morphology can still be tested as can the biogeographic origins of the lineage.

Our results indicate that there have confidently been at least eight independent shifts to hummingbird pollination from a bee-pollinated ancestor, with the strongest evidence pointing to nine total shifts. All analyses strongly support *Costus stenophyllus*, with an ornithophilous morphology, as sister to the remaining Neotropical taxa suggesting that this early-diverging lineage evolved hummingbird pollination independently from other hummingbird pollinated species. Further studies investigating the developmental genetics and morphometrics of floral traits associated with bird pollination across *Costus* will help define the particular characters involved in the hummingbird pollination trait, and define how these characters might evolve to produce the complex morphologies associated with the bird pollination syndrome.

Several unresolved areas of the phylogeny impeded our ability to conclusively state the total number of character state transitions for the complex pollination syndrome character; however, the support for nodes at which transitions occurred is significant and indicates that we have arrived at a conservative number of potential shifts for the genus. In analyses performed on the ML tree, all shifts to hummingbird pollination shown are statistically significant and nodes are well supported save the *C. zingiberoides*/*C. woodsonii* clade (Fig. 2), which was found in 51% of the 707,000 most parsimonious trees; all extant species of this clade, however, are ornithophilous and are the result of a single evolution of the bird pollination syndrome. The relationship between the *C. asplundii*/*C. arabicus* and *C. quasi-appendiculatus*/*C. woodsonii* clade is still uncertain, as is the relationship between *C. laevis*/*C. wilsonii* and *C. lasius*/*C. allenii*, yet the clades themselves are well supported and indicate the occurrence of multiple, independent shifts to the ornithophilous morphology from a bee-pollinated ancestral form regardless of their placement. The placement of the *C. vinosus*/*C. beckii* clade is still unclear: attempts to infer the effect of this phylogenetic uncertainty on the hypothesized number of shifts in pollination morphology were also inconclusive due to low support for a reconstruction of bee pollination for the most recent common ancestor of *C. beckii* and *C. woodsonii* (Table 4) in addition to the polytomy present in the *C. laevis*/*C. woodsonii* clade. Ancestral state reconstruction for pollination syndrome performed on the Bayesian tree had lower support all around, suggesting that the phylogenetic uncertainty found in the polytomies confounded ancestral state reconstruction attempts.

This is the first study to demonstrate there has been a toggle in pollination morphology, with reversals back to the ancestral bee pollination morphology occurring in the *C. dirzoi*/*C. lima* clade. The monophyly of the pollination-syndrome-toggling *C. dirzoi*/*C. lima* clade is very strongly supported with all methods. The ancestral state is strongly supported as hummingbird pollination morphology with the Bayesian and the Mesquite likelihood reconstructions (and moderately supported with BayesTraits likelihood reconstruction), and there is strong support for the ancestral character state reconstructions for nodes within this clade (Tables 3, 4). With only the phylogenetic placement of *C. longibracteolatus* remaining to be clarified, this clade clearly shows reversals to melittophilous morphologies after

an initial evolution of ornithophilous morphology. While there appear to have been eight or nine independent origins of an ornithophilous floral form, there are fewer reversals to a melittophilous morphology, all of which occur in the *C. dirzoi/C. lima* clade.

Ancestral area reconstruction analyses all strongly support a Mexican/Central American point of dispersal to the New World with the highest probability of arrival occurring along the Pacific Coast. Further dating analyses are required to discuss the biogeographic history of this group and the effect of distribution on speciation, as temporal evidence is needed to discuss past biogeographic scenarios (Crisp et al. 2011). We can, however, discuss the results here in the light of prior work. If the previous fossil calibrated dating is assumed and the Neotropical radiation occurred around 22 ma, then biogeographic upheavals such as the Andean uplift (~10 ma) and the near closure of the Isthmus of Panama [recently shown to be earlier than thought at about 15 ma (Montes et al. 2012) or perhaps even 31–16 ma (Bacon et. Al. 2013)], would certainly have played an important role in speciation through vicariance. Additionally, at that time there were few Costaceae taxa as part of the flora of the Neotropics, suggesting that intra-lineage competition may not have had a strong effect on diversification (Specht 2005). This could support the hypothesis that changing geography pushed populations into higher elevations better populated by hummingbirds, leading to floral forms that resulted in specific pollination syndromes leading to reproductive isolation. This hypothesis is further supported by the positive support for a weak correlation between elevation and pollination syndromes shown here with current distributions. If, however, the ITS molecular clock dating is assumed, with a Neotropical radiation at around four ma (Kay et al. 2005), the factors influencing diversification may be quite the opposite, with less geographic and climatic upheaval and more competition among Zingiberales taxa or other bird/bee pollinated plants driving extremely rapid rates of diversification.

The sister clade to *Costus*, a South American clade consisting of *Chamaecostus* (seven species), *Monocostus* (one species), and *Dimerocostus* (three to five species), would have experienced a similar biogeographic history, yet failed to diversify either taxonomically or morphologically to the extent of the diversity exemplified by *Costus*. These three genera comprise species that lack the extreme pollination-specific morphologies associated with the Neotropical *Costus* clade. Such data support our hypothesis that the rapid radiation observed in Neotropical *Costus* is correlated with the specialized pollination morphologies characteristic of this lineage. An expanded Costaceae phylogeny with outgroup fossil dating is needed to revisit these questions, and may provide greater insight into the biogeography of this group and the impact of pollinator-mediated vs. vicariance-related speciation through means of reproductive isolation and their combined effect on diversification rates.

Acknowledgments. The authors thank Dr. Paul J. M. Maas and Hiltje Maas for their shared expertise in Costaceae systematics; Y. Wang, I. Liao, H. Cooper, L. Lagomarsino, K. Yu, B. Wong, and A. Almeida for generating sequence data; Members of the Specht Lab, especially A. Almeida and R. Yockteng for helpful comments on data generation, analysis and manuscript preparation. Funding for this project was provided by the National Geographic Society #8994-11 and UC Berkeley CNR-BSP, SPUR, and URAP.

Literature Cited

Bacon, C. D., A. Mora, W. L. Wagner, and C. A. Jaramillo. 2013. Testing geological models of evolution of the Isthmus of Panama in a phylogenetic framework. *Botanical Journal of the Linnean Society* 171: 287–300.

Baldwin, B. G. and S. Markos. 1998. Phylogenetic utility of the external transcribed spacer (ETS) of 18S–26S rDNA: Congruence of ETS and ITS trees of *Calycadenia* (Compositae). *Molecular Phylogenetics and Evolution* 10: 449–463.

Baum, D., R. Small, and J. Wendel. 1998. Biogeography and floral evolution of baobabs (*Adansonia* Bombacaceae) as inferred from multiple data sets. *Systematic Biology* 47: 181–207.

Crisp, M. D., S. A. Trewick, and L. G. Cook. 2011. Hypothesis testing in biogeography. *Trends in Ecology & Evolution* 26: 66–72.

Darriba, D., G. L. Taboada, R. Doallo, and D. Posada. 2012. jModelTest 2: More models, new heuristics and parallel computing. *Nature Methods* 9: 772.

Edwards, K., C. Johnstone, and C. Thompson. 1991. A simple and rapid method for the preparation of plant genomic DNA for PCR analysis. *Nucleic Acids Research* 19: 1349.

Guindon, S., J. F. Dufayard, V. Lefort, M. Anisimova, W. Hordijk, and O. Gascuel. 2010. New algorithms and methods to estimate maximum-likelihood phylogenies: Assessing the performance of PhyML 3.0. *Systematic Biology* 59: 307–331.

Johansen, L. B. 2005. Phylogeny of *Orchidantha* (Lowiaceae) and the Zingiberales based on six DNA regions. *Systematic Botany* 30: 106–117.

Kay, K. M. 2006. Reproductive isolation between two closely related hummingbird-pollinated Neotropical gingers. *Evolution* 60: 538–552.

Kay, K. M. and D. W. Schemske. 2003. Pollinator assemblages and visitation rates for 11 species of Neotropical *Costus* (Costaceae). *Biotropica* 35: 198–207.

Kay, K. M., P. A. Reeves, R. G. Olmstead, and D. W. Schemske. 2005. Rapid speciation and the evolution of hummingbird pollination in Neotropical *Costus* subgenus *Costus* (Costaceae): Evidence from nrDNA ITS and ETS sequences. *American Journal of Botany* 92: 1899–1910.

Maddison, W. P. and D. R. Maddison. 2006. StochChar: A package of Mesquite modules for stochastic models of character evolution. Version 1.1 Available from http://mesquiteproject.org.

Maddison, W. P. and D. R. Maddison. 2011. Mesquite: A modular system for evolutionary analysis. Version 2.75 Available from http://mesquiteproject.org.

Miller, M. A., W. Pfeiffer, and T. Schwartz. 2010. Creating the CIPRES science gateway for inference of large phylogenetic trees. New Orleans, Louisiana: Proceedings of the Gateway Computing Environments Workshop (GCE).

Montes, C., A. Cardona, R. McFadden, S. E. Morón, C. A. Silva, S. Restrepa-Moreno, D. A. Ramírez, N. Hoyos, J. Wilson, D. Farris, G. A. Bayona, C. A. Jaramillo, V. Valencia, J. Bryan, and J. A. Flores. 2012. Evidence for middle Eocene and younger land emergence in central Panama: Implications for Isthmus closure. *Geological Society of America Bulletin* 124: 780–799.

Olson, D. M., E. Dinerstein, E. D. Wikamanayake, N. D. Burgess, G. V. N. Powell, E. C. Underwood, J. A. D'Amico, I. Itoua, H. E. Strand, J. C. Morrison, C. J. Loucks, T. F. Allnutt, T. H. Ricketts, Y. Kura, J. F. Lamoreux, W. W. Wettengel, P. Hedao, and K. R. Kassem. 2001. Terrestrial ecoregions of the world: A new map of life on Earth. *Bioscience* 51: 933–938.

Paradis, E., J. Claude, and K. Strimmer. 2004. APE: Analyses of phylogenetics and evolution in R language. *Bioinformatics* 20: 289–290.

Pagel, M. 1999. The maximum likelihood approach to reconstructing ancestral character states of discrete characters on phylogenies. *Systematic Biology* 48: 612–622.

Pagel, M. and A. Meade. 2004a. BayesTraits. Available from http://www.evolution.rdg.ac.uk.

Pagel, M., A. Meade, and D. Barker. 2004. Bayesian estimation of ancestral character states on phylogenies. *Systematic Biology* 53: 673–684.

Plummer, M., N. Best, K. Cowles, and K. Vines. 2006. CODA: Convergence diagnosis and output analysis for MCMC. *R News* 6: 7–11.

Rabosky, D. L. 2014. Automatic detection of key innovations, rate shifts, and diversity-dependence on phylogenetic trees. *PLoS ONE* 9: e89543, doi: 10.1371/journal.pone.0089543.

Rabosky, D. L., M. Grundler, C. Anderson, P. Title, J. J. Shi, J. W. Brown, H. Huang, and J. G. Larson. 2014. BAMMtools: An R package for the analysis of evolutionary dynamics on phylogenetic trees. *Methods in Ecology and Evolution*. Doi: 10.1111/2041-210X.12199.

Rambaut, A. and A. J. Drummond. 2007. Tracer v1.5, Available from http://tree.bio.ed.ac.uk/software/tracer/.

Ronquist, F. and J. P. Huelsenbeck. 2003. MRBAYES 3: Bayesian phylogenetic inference under mixed models. *Bioinformatics* 19: 1572–1574.

Sakai, S., M. Kato, and T. Inoue. 1999. Three pollination guilds and variation in floral characteristics of Bornean gingers (Zingiberaceae and Costaceae). *American Journal of Botany* 86: 646–658.

Shaw, J., E. B. Lickey, E. E. Schilling, and R. Small. 2007. Comparison of whole chloroplast genomes sequences to choose noncoding regions for phylogenetic studies in angiosperms: The tortoise and the hare III. *American Journal of Botany* 94: 275–288.

Smith, J. F. 2000. Phylogenetic signal common to three data sets: Combining data which initially appear heterogeneous. *Plant Systematics and Evolution* 221: 179–198.

Specht, C. D. 2005. Phylogenetics, floral evolution, and rapid radiation in the tropical Monocotyledon family Costaceae (Zingiberales). *Plant Genome Biodiversity and Evolution* 1B: 29–60.

Specht, C. D. 2006a. Systematics and evolution of the tropical monocot family Costaceae (Zingiberales): A multiple dataset approach. *Systematic Botany* 31: 89–106.

Specht, C. D. 2006b. Gondwanan vicariance or dispersal in the tropics? The biogeographic history of the tropical monocot family Costaceae (Zingiberales). Pp. 631–642 in *Monocots: Comparative biology and evolution*. eds. J. T. Columbus, E. A. Friar, C. W. Hamilton, J. M. Porter, L. M. Prince, and M. G. Simpson. Claremont, California: Rancho Santa Ana Botanic Garden.

Specht, C. D., W. J. Kress, D. W. Stevenson, and R. DeSalle. 2001. A molecular phylogeny of Costaceae (Zingiberales). *Molecular Phylogenetics and Evolution* 21: 333–345.

Swofford, D. L. 2003. PAUP*. Phylogenetic analysis using parsimony (*and other methods). Version 4. Sunderland: Sinauer Associates.

Taberlet, P., L. Gielly, G. Pantou, and J. Bouvet. 1991. Universal primers for amplification of three non-coding regions of chloroplast DNA. *Plant Molecular Biology* 17: 1105–1109.

Thomson, J. D. and P. Wilson. 2008. Explaining evolutionary shifts between bee and hummingbird pollination: Convergence, divergence and directionality. *International Journal of Plant Sciences* 169: 23–38.

White, T. J., T. Bruns, S. Lee, and J. Taylor. 1990. Amplification and direct sequencing of fungal ribosomal RNA genes for phylogenetics. Pp. 315–322 in *PCR protocols: A guide to methods and applications*. eds. M. Innis, D. Gelfand, J. Sninsky, and T. White. San Diego: Academic Press.

Yu, Y., A. J. Harris, and X. J. He. 2010. S-DIVA (statistical dispersal-vicariance analysis): A tool for inferring biogeographic histories. *Molecular Phylogenetics and Evolution* 56: 848–850.

Yu, Y., A. J. Harris, and X. J. He. 2012. RASP (reconstruct ancestral state in phylogenies), v. 2.1b. Available at http://mnh.scu.edu.cn/soft/blog/RASP.

Appendix 1. Voucher Information for species sampled and GenBank accession numbers for DNA sequences. Information is as follows: species name, *voucher information*, GenBank accession numbers for five loci: ITS, ETS, *CaM*, *rsp16*, *trnL-f*. GenBank accessions beginning KJ were created in this study. Previously generated sequences for a species that used a separate vouchered individual have the voucher information indicated in parentheses. Dashes denote missing data. Collector abbreviations for herbarium vouchers: BS = B. Stahl; BTM = B. T. Meise; CS = Chelsea Specht; M = P. J. M. Maas; Mood = John Mood; KMN = Lyon Arboretum Herbarium (HLA) collector Ken Nagata; R = David Skinner; TvA = Tinde van Andel; US = Uwe Scharf; WJK = W. John Kress. Abbreviations for living collections: NMNH = Smithsonian Greenhouse Collections; L = Lyon Arboretum; BB = Burgers Bush; NY = New York Botanical Garden Living Collection; RB = Rio de Janeiro Botanical Garden herbarium collections.

Chamaecostus lanceolatus (Petersen) var. ***pulchriflorus*** (Ducke) C. D. Specht & D. W. Stev. *RB550388*, KJ011475, KJ011224, KJ011299, KJ011419, KJ011347; ***Chamaecostus cuspidatus*** (Nees & Mart.) C. D. Specht & D. W. Stev., *RB584184*, AY994739 (*WJK94-3681*), KJ011223, KJ011298, KJ011418, KJ011346; ***Chamaecostus subsessilis*** (Nees & Mart.) C. D. Specht & D. W. Stev. *RB584183*, KJ011476, KJ011225, KJ011300, KJ011420, KJ011348; ***Hellenia globosa*** (Blume) S.R. Dutta, *CS02-351* as ***Cheilocostus globosus***, KJ011479, KJ011228, -, KJ011423, AY994592 (*Mood 1713*); ***Costus afer*** Ker Gawl., *M10205*, KJ011425, KJ011151, KJ011230, KJ011351, KJ011304; ***Costus albiflos*** Maas & H. Maas , *M9968*, KJ011426, KJ011152, KJ011231, KJ011352, KJ011305; ***Costus allenii*** Maas, *M9563*, AY994743 (*NY347/95A*), KJ011153, -, KJ011353, AY994587 (*NY347/95A*); ***Costus amazonicus*** J. F. Macbr., *M9036*, AY994742 (*CS02-327*), KJ011154, KJ011232, KJ011354, AY994586 (*CS02-327*); ***Costus arabicus*** L., *CS98-193*, AY041034, KJ011155, KJ011233, KJ011355, KJ011306; ***Costus asplundii*** (Maas) Maas, *R2976*, KJ011427, KJ011156, KJ011234, KJ011356, KJ011307; ***Costus barbatus*** Suess., *CS01-256*, AY994741 (*NY1413/91B*), KJ011157, KJ011235, KJ011357, KJ011308; ***Costus beckii*** Maas & H. Maas, *CS99-232*, KJ011428, KJ011158, KJ011236, KJ011358, KJ011309; ***Costus bracteatus*** Rowlee, *M9409*, KJ011429, KJ011159, KJ011237, KJ011359, KJ011310; ***Costus chartaceus*** Maas, *WJK90-3124*, AY994719 (*WJK99-6356*), KJ011160, KJ011238, KJ011360, AY994559 (*WJK 99-6356*); ***Costus claviger*** Benoist, *M9306*, AY994740 (*KMN2361*), KJ011161, KJ011239, KJ011361, AY994584 (*KMN 2361*); ***Costus comosus*** var. ***bakeri*** (K. Schum.) Maas, *BB1999-0126011*, KJ011430, KJ011162, KJ011240, KJ011362, KJ011311; ***Costus curvibracteatus*** Maas, *M9381*, KJ011431, KJ011163, KJ011241, KJ011363, AY994583 (*NY356-95A*); ***Costus deistelii*** K. Schum., *M9298*, AY994752, KJ011165, KJ011242, KJ011365, AY994599; ***Costus*** aff. ***dubius***, *L92.0048*, KJ011434, KJ011167, KJ011244, KJ011367, AY994596 (*M3549*); ***Costus dinklagei*** K. Schum., *TvA3549*, KJ011433, KJ011166, KJ011243, KJ011366, KJ011312; ***Costus dirzoi*** García-Mend. & Ibarra-Manr., *1996-0228002*, KJ011435, KJ011168, KJ011245, KJ011368, KJ011313; ***Costus dubius*** K. Schum., *M10206*, KJ011436, KJ011169, KJ011246, KJ011369, KJ011314; ***Costus erythrocoryne***, K. Schum., AY994738 (*CS02-326*), AY972950 (*KK98.73*), -, -, AY994579 (*CS02-326*); ***Costus erythrophyllus*** Loes., *R2847*, KJ011437, KJ011170, KJ011247, -, KJ011315; ***Costus erythrothyrsus*** Loes., *M9317*, KJ011438, KJ011171, KJ011248, KJ011370, KJ011316; ***Costus gabonensis*** Koechlin, *M10291*, KJ011439, KJ011172, KJ011249, KJ011371, KJ011317; ***Costus geothyrsus*** K. Schum., *BS6782*, KJ011440, KJ011173, KJ011250, KJ011372, KJ011318; ***Costus glaucus*** Maas, *Delft 46-325*, KJ011441, KJ011174, KJ011251, KJ011373, KJ011319; ***Costus guanaiensis*** var. ***guanaiensis*** Rusby, *R2666*, AY994737 (*L94.0306*), KJ011175, KJ011252, KJ011374, AY994577 (*L94.0306*); ***Costus guanaiensis*** var. ***macrostrobilus*** (K. Schum.) Maas, *CS00-253*, KJ011442, KJ011176, KJ011253, KJ011375, KJ011320; ***Costus guanaiensis*** var. ***tarmicus*** (Loes.) Maas, *KMN2811*, AY994751, KJ011177, KJ011254, KJ011376, AY994597; ***Costus laevis*** Ruiz & Pav., *CS01-257*, KJ011443, KJ011178, KJ011255, KJ011377, AY994576 (*NY351/95A*); ***Costus lasius*** Loes., *M9155*, AY994735 (*NMNH 94-670*), KJ011179, -, KJ011378, AY994575 (*NMNH 94-670*); ***Costus lateriflorus*** Gagnep., *M10331*, KJ011444, KJ011180, KJ011256, KJ011379, KJ011321; ***Costus letestui*** Pellegr., *CS02-331*, AY994733, KJ011181, KJ011257, KJ011380, AY994573; ***Costus leucanthus*** Maas, *BB1996-1105001*, KJ011445, KJ011182, KJ011258, KJ011381, KJ011322; ***Costus*** aff. ***ligularis***, *BB1998-0923003*, KJ011446, KJ011183, KJ011259, KJ011382, KJ011323; ***Costus*** aff. ***ligularis***, *M10226*, KJ011448, KJ011185, KJ011261, KJ011384, -; ***Costus*** aff. ***ligularis*** , *US237*, KJ011447, KJ011184, KJ011260, KJ011383, KJ011324; ***Costus* sp. nov**., *M9995*, KJ011449, KJ011186, KJ011262, KJ011385, KJ011325; ***Costus lima*** K. Schum., *R3014*, KJ011450, KJ011187, KJ011263, KJ011386, -; ***Costus lima*** var. ***scabremarginatus*** Maas, *BTM75-0400*, KJ011451, KJ011188, KJ011264, KJ011387, KJ011326; ***Costus loangensis*** H. Maas & Maas, *M10184*, KJ011452, KJ011189, KJ011265, KJ011388, KJ011327; ***Costus longibracteolatus*** Maas, *R3003*, KJ011453, KJ011190, KJ011266, KJ011389, KJ011328; ***Costus lucanusianus*** J. Braun & K. Schum., *M10000*, KJ011455, KJ011192, KJ011268, KJ011391, -; ***Costus maboumiensis*** Pellegr., *M10227*, KJ011456, KJ011193, KJ011269, KJ011392, KJ011330; ***Costus*** aff. ***afer***, *WJK94-3683*, AY994731, KJ011194, KJ011270, KJ011393, AY994571; ***Costus malortieanus*** H. Wendl., *M9791*, KJ011457, KJ011195, KJ011271, KJ011394, KJ011331; ***Costus montanus*** Maas, *R2972*, AY994729 (*KKsn*), KJ011196, -, -, AY994569 (*KKsn*); ***Costus nitidus*** Maas, *M9524*, KJ011458, KJ011197, KJ011272, -, KJ011332; ***Costus osae*** Maas & H. Maas, *M9501*, KJ011459, KJ011198, KJ011273, KJ011395, KJ011333; ***Costus phaeotrichus*** Loes., *CS02-323*, AY994721, KJ011199, KJ011274, KJ011396, AY994561; ***Costus*** aff. ***phyllocephalus***, *BB870057*, KJ011460, KJ011200, KJ011275, KJ011397, KJ011334; ***Costus*** aff. ***phyllocephalus***, *M10389*, KJ011461, KJ011201, KJ011276, KJ011398, KJ011335; ***Costus pictus*** D.Don ex Lindl., *WJK94-3691*, AY994726, KJ011202, KJ011277, KJ011399, AY994566; ***Costus plicatus*** Maas, *WJK94-5376*, AY994725, KJ011203, KJ011278, KJ011400, AY994565; ***Costus productus*** Gleason ex Maas, *R2693*, KJ011462, KJ011204, KJ011279, KJ011401, KJ011336; ***Costus pulverulentus*** C. Presl, *WJK94-3680*, AY994723, KJ011205, KJ011280, KJ011402, AY994563; ***Costus quasi-appendiculatus*** Woodson ex Maas, *CS99-233*, KJ011463, KJ011206, KJ011281, KJ011403, KJ011337; ***Costus ricus*** Maas & H. Maas, *R2970*, KJ011464, KJ011207, KJ011282, KJ011404, KJ011338; ***Costus scaber*** Ruiz & Pav., *R2253*, KJ011465, KJ011208, KJ011283, KJ011405, KJ011339;

Costus spectabilis K. Schum., *WJK97-6118*, AY994718, KJ011209, -, KJ011406, AY994556; ***Costus spicatus*** Sw., *WJK02-7143*, KJ011432, KJ011164, KJ011284, KJ011364, KJ011340; ***Costus spiralis*** Roscoe, *M9335*, KJ011466, KJ011210, KJ011285, KJ011407, -; ***Costus stenophyllus*** Standl. & L. O. Williams, *L75.0305*, KJ011467, KJ011211, KJ011286, KJ011408, AY994560 (*CS02-313*); ***Costus talbotii*** Ridl., *2003-0109009*, KJ011471, KJ011216, KJ011291, KJ011412, KJ011343; ***Costus*** aff. ***tappenbeckianus***, *WJK94-3697*, AY994715, KJ011215, KJ011290, -, AY994553; ***Costus*** aff. ***tappenbeckianus***, *TvA3675*, KJ011468, KJ011212, KJ011287, KJ011409, -; ***Costus*** aff. ***tappenbeckianus***, *US235*, KJ011469, KJ011213, KJ011288, KJ011410, KJ011341; ***Costus*** aff. ***tappenbeckianus***, *US236*, KJ011470, KJ011214, KJ011289, KJ011411, KJ011342; ***Costus varzearum*** Maas, *WJK94-5379*, AY994722, KJ011217, KJ011292, KJ011413, AY994551 (*CS01-277*); ***Costus villosissimus*** Jacg., *KMN632*, AY994713, KJ011218, KJ011293, KJ011414, AY994550; ***Costus vinosus*** Maas, *M9568*, KJ011472 (*WJK94-3727*), KJ011219, KJ011294, -, KJ011344; ***Costus wilsonii*** Maas, *M9507*, KJ011473, KJ011220, KJ011295, KJ011415, -; ***Costus woodsonii*** Maas, *CS01-264*, AY994712, KJ011221, KJ011296, KJ011416, AY994549; ***Costus*** aff. ***lucanusianus*** (yellow flower form), *Breteler5297*, KJ011454, KJ011191, KJ011267, KJ011390, KJ011329; ***Costus zingiberoides*** J. F. Macbr., *BTM86-00-01*, KJ011474, KJ011222, KJ011297, KJ011417, KJ011345; ***Dimerocostus strobilaceus*** Kuntze, *CS01-272*, KJ011478, KJ011227, KJ011302, KJ011422, KJ011350; ***Monocostus uniflorus*** (Peterson) Maas, *WJK75-0065*, KJ011477, KJ011226, KJ011301, KJ011421, KJ011349; ***Tapeinochilos queenslandiae*** K. Schum., *DavisB68.168*, KJ011480, KJ011229, KJ011303, KJ011424, AY994542 (*Hay7052*)